Eur. Phys. J. C 11, 717–728 (1999)
Digital Object Identifier (DOI) 10.1007/s100529900237

THE EUROPEAN PHYSICAL JOURNAL C
© Springer-Verlag 1999

Flavour symmetry of mesonic decay couplings

E. van Beveren[1], G. Rupp[2]

[1] Departamento de Física, Universidade de Coimbra, 3000 Coimbra, Portugal (eef@malaposta.fis.uc.pt)
[2] Centro de Física das Interacções Fundamentais, Instituto Superior Técnico, Edifício Ciência, 1096 Lisboa Codex, Portugal (george@ajax.ist.utl.pt)

Received: 8 January 1999 / Revised version: 19 April 1999 / Published online: 16 November 1999

Abstract. We present flavour-symmetric results for the OZI-allowed couplings of quark–antiquark systems to meson–meson channels in the harmonic-oscillator expansion. We tabulate their values for all possible open and closed decay channels of pseudoscalar, vector, and scalar mesons. We compare the predictions of a model that employs these flavour-symmetric couplings, both with the results of a model which uses explicitly flavour-dependent couplings, and with experiment.

1 Introduction

Particle interactions are described by point-particle vertices in fundamental theories. Quarks, the basic particles for strong interactions, are point objects, to the best of our knowledge. Hence they are assumed to interact via point-particle vertices in the existing theories: through a quark–gluon vertex in quantum chromodynamics (QCD) [1], through a four-quark vertex in the Nambu–Jona–Lasinio model (NJL) [2].

QCD exhibits good agreement with experiment, qualitatively for low and medium energies, and, moreover, quantitatively at high energies [3], whereas NJL shows good agreement with experiment only for energies below 1 GeV [4]. So in the energy interval crucial to meson physics, i.e., ranging from the two-pion threshold to energies as high as the states in the bottomonium system, no fundamental theory possesses a satisfactory descriptive power: QCD does not, because the relevant momentum transfers are too low and thus the effective colour coupling constant is too large for a perturbative approach, and NJL does not, because the energies are too high. Consequently, for a quantitative description of the spectra and scattering of mesons and baryons, neither of the two theories has sufficient predictive power for the time being. Therefore, the use of quark models is still opportune in this domain of hadronic physics.

Now, ideally a quark model should be derived from QCD, but this is rather utopian as yet. As a matter of fact, not even a direct relation between QCD and confinement has been established and so confinement usually has to be imposed on the valence quarks of the model [5]. Different models follow distinct strategies to achieve this, and the manner in which confinement is approached distinguishes the models among each other. Moreover, each model has its own very specific purpose, often not mentioned in too much detail by the authors, which makes it difficult to compare models. For instance, there exist heavy-quark potential models made to measure in order to reproduce, with great accuracy, the radial and angular spectra of charmonium and bottomonium, as well as the electromagnetic properties of these systems. But if the same potentials are used in the light quark sector, the results are normally quite bad, especially for radial excitations, and even possible relativistic corrections are insufficient to cure the discrepancies. Conversely, sophisticated relativistic models for the light mesons usually fail to reproduce the correct radial spacings in the charmonium and bottomonium spectra.

On the other hand, most quark models treat hadrons as manifestly stable bound states of quarks, simply ignoring the fact that most hadrons are resonances, some of them even extremely broad, so as to make their very existence questionable. Among the few exceptions, we should mention the systematic inclusion of open and closed strong decay channels in the Helsinki unitarised quark model (HUQM) [6] and the Nijmegen unitarised meson model (NUMM) [7], and further the coupled-channel approach of Eichten and collaborators to charmonium [8] and bottomonium [9]. Also of interest are a very recent improved adiabatic formalism allowing a systematic low-energy expansion of the impact of thresholds on the hadronic spectra, and a chiral confining model for scalar mesons [10].

The standard justification for ignoring strong decay is the conjecture that its effect will be to produce predominantly imaginary mass shifts, thus allowing to first fit the real parts of the spectra and then to treat the hadronic widths *a posteriori*, with perturbative methods. However, we know from fundamental principles in scattering theory that real shifts are generally of the same order as or even larger than the imaginary ones. Moreover, hadronic loops, i.e., *virtual decay channels*, give rise to *attractive forces*, so that the shifts due to, in principle, all closed decay channels must be added up, so as to produce a negative mass

shift. So not even the true bound states can be treated as pure quark states. The usual excuse is the unsupported assertion that the effect of closed channels will be negligible, except near threshold.

However, the NUMM, devised to simultaneously describe meson spectra and meson–meson scattering, from the light pseudoscalars and vectors [7], via the usually awkward scalars [11], all the way up to the $c\bar{c}$ and $b\bar{b}$ sectors [12], showed that both premises are indeed wrong: real shifts are generally comparable with or larger than the imaginary ones, and the damping of closed channels is insufficient to make their influence on the ground states of the spectra negligible. On the contrary, due to the nodal structure of the radial wave functions and the mentioned additivity property, the shifts – real and negative – of the ground states are usually largest [13]. Furthermore, no drastic enhancement takes place near threshold, so that these states cannot be singled out [14].

Having come to the conclusion that, for a truly quantitative description of the mesonic spectra, one must include the coupling to meson–meson channels; the crucial questions to be raised are how to calculate the involved coupling constants and which two-meson channels to take along. Here, one should step back and have another look at the QCD Lagrangian. Realising that, at least qualitatively, there should be no obvious disagreement between QCD and whatever meson model to be used, we are led to respect manifest flavour blindness. This will impose stringent conditions on how couplings can be computed and how to select classes of decay channels, since obviously one cannot take into account an infinite number of these.

Models which describe the scattering of mesons (and/or baryons) often imitate the fundamental theories in the sense that interactions take place via effective point-particle vertices. However, mesons (and baryons) are composite systems, built out of strongly interacting valence quarks, glue, and a quark–antiquark sea. So it seems obvious that, when mesons (and baryons) are considered point objects, some information must get lost. In this paper we will demonstrate that this can indeed be the case, and we consider how this makes itself manifest in the flavour non-independence of the strong interactions thus described, when not dealt with carefully.

Point interactions are a powerful tool in constructing theories that not only consider relativistic kinematics, but also take into account the property of particle creation and annihilation. However, in applying point interactions to composite systems, one should include all hidden degrees of freedom. Flavour is just one such degree of freedom. Angular momentum and spin are others which should be properly included. At present, it is opportune to model the internal degrees of freedom and next to integrate them out for the determination of the effective point couplings. A consistent way of doing so in the framework of the $^3P_0$ model, which moreover preserves flavour independence, is described below. For the origins and some key aspects of the $^3P_0$ model, see [15].

The organisation of this paper is as follows. In Sect. 2, we discuss the general philosophy behind a simple model for flavour independence. This model is then exposed in Sect. 3. The intensities of the three-meson vertices for meson decay into meson–meson pairs are given in Sect. 4. Results are discussed in Sect. 5. The consequences of flavour (in)dependence are studied for two different, though similar, models in Sect. 6. Some essential formulae are collected in the Appendices A and B.

2 Flavour independence

Since strong interactions are independent of flavour (see [16] for a recent experimental confirmation), the probability to create a quark–antiquark pair out of the vacuum cannot depend on the flavour of the quark and the antiquark. However, it obviously depends on the masses involved. But if for a moment we assume that the flavour masses, or at least the effective quark masses in the relevant energy interval of the three lowest flavours, *up*, *down* and *strange*, are equal, then the corresponding probabilities of pair creation should be equal. Let us apply this principle to the strong coupling of a meson to a pair of mesons. Here, we assume that the related strong decay processes are triggered by the creation of a flavourless quark–antiquark pair.

In order to set the picture, we consider a simple model in which the initial meson is described by a confined quark–antiquark system of any flavour, given by

$$a\bar{b}, \tag{1}$$

where a and b represent any of the three flavours under discussion, and the final pair of OZI allowed decay products is described by a system of two freely moving mesons, which represent any of the three combinations

$$(a\bar{u})+(u\bar{b})\,, \quad (a\bar{d})+(d\bar{b})\,, \quad (a\bar{s})+(s\bar{b})\,. \tag{2}$$

Also, let us, for a moment, assume that no further quantum numbers are involved. Then, flavour blindness of the strong interactions demands that the probabilities are equal for the $a\bar{b}$ system to decay into any of the three channels of (2). In particular, when under full flavour symmetry the six mesons represented in (2) all have the same mass, then the experimental results for the decay of system (1) into any of the three channels of (2) should be indistinguishable.

Let the three decay coupling constants of the process under consideration be represented by, respectively,

$$g(a,b;u), \quad g(a,b;d), \quad g(a,b;s). \tag{3}$$

Then, assuming flavour independence, we have the identities

$$\{g(a,b;u)\}^2=\{g(a,b;d)\}^2=\{g(a,b;s)\}^2\,, \tag{4}$$

and, moreover, for the total decay intensity $\Gamma(a,b)$ the relation

$$\Gamma(a,b)=A\left[\{g(a,b;u)\}^2+\{g(a,b;d)\}^2 +\{g(a,b;s)\}^2\right], \tag{5}$$

where the proportionality factor A is also completely flavour symmetric, which means constant here. Furthermore, one has that, under flavour symmetry, $\Gamma(a,b)$ must be independent of the flavours a and b.

Unfortunately, quarks are fermions and mesons are spatially extended systems, and hence spin and spatial quantum numbers do play an important role in the decay of a meson into a pair of mesons. Nevertheless, it remains possible to construct coupling constants which have the property that the total decay probability is independent of the flavour of the decaying meson in the limit of equal masses, as we will see below.

3 Modeling full flavour symmetry

When a normalised wave function ψ is expanded on a complete orthonormal basis ϕ_n, for $n = 0, 1, 2, \ldots$, according to

$$\psi = \sum_{n=0}^{\infty} c_n \phi_n, \tag{6}$$

one has for the expansion coefficients c_n the property

$$\sum_{n=0}^{\infty} |c_n|^2 = 1. \tag{7}$$

It is exactly property (7) that leads to flavour independence.

Let us consider a system of two quarks and two antiquarks, like any of the three combinations of (2). One complete basis for the Hilbert space of such a system can be constructed by taking products of the internal wave function of the $a\bar{b}$ system, specifying thereby its internal spatial and flavour quantum numbers, the internal wave function of the $q\bar{q}$ (either $u\bar{u}$, $d\bar{d}$ or $s\bar{s}$) system, and the relative wave function of the two subsystems. Another complete basis for this Hilbert space consists of products of the internal wave function of the $a\bar{q}$ system, the internal wave function of the $q\bar{b}$ system, and the relative wave function of those two subsystems. Any wave function describing one of the two-quark–two-antiquark systems (2) can be expanded in either of the bases defined above.

Such an expansion takes a particularly manageable form if the four partons are supposed to move in a harmonic oscillator potential with universal frequency. In that case the spatial quantum numbers are linearly related to the total energy of the system, which gives rise to finite bases at each energy level and hence to finite expansions. The flavour-symmetry condition (7) then becomes a finite sum, which makes it easy for verification. Furthermore, the restriction to harmonic oscillators is not a real limitation, since any other basis can always be expanded in the corresponding harmonic-oscillator basis, $\{n\}$, according to

$$\langle M_1 M_2 \,|V|\, M\rangle = \sum_{\{n,n'\}} \langle M_1 M_2 \,|n'\rangle \,\langle n' \,|V|\, n\rangle \,\langle n \,|M\rangle \,. \tag{8}$$

Here, V represents the interaction Hamiltonian which describes the transitions between the quark–antiquark system $a\bar{b}$ and the two-meson channels. We assume that the spatial, or momentum-dependent, part of the matrix elements $\langle n' \,|V|\, n\rangle$ is flavour independent and that the flavour-dependent parts are constants.

The expansion of a particular many-particle wave function into a specific basis for well-defined subsystems, or *recoupling*, has been studied a great deal in the past. The related coefficients for the harmonic-oscillator basis are known as *Moshinsky brackets*. Moshinsky brackets are well-known coefficients of recoupling in nuclear physics; see [17] for their definition. The group-theoretical implications of parton recoupling in the harmonic-oscillator approximation have been studied exhaustively in [18]. Their application to meson decay has for the first time been formulated in [19]. A full generalisation for the spatial part of the recoupling constants, which includes all possible quantum numbers for any number of (bosonic) partons, can be found in [20]. The inclusion of fermionic and flavour degrees of freedom, which leads to an analytic expression for the coupling constants of any meson to any of its two-meson real or virtual decay channels, is given in [21], for the case that the new valence pair is created with $^3P_0$ quantum numbers. A Fortran source program is available on request.

4 Coupling constants for three-meson vertices

Within the formalism outlined above, we assume that mesons can be classified by the quantum numbers of their valence constituent quark–antiquark distributions, i.e.,

$$\text{meson}\,(j, M, \ell, s, n, \mathcal{M})\,. \tag{9}$$

The quantum numbers j and M in (9) represent, respectively, the spin of the meson and its z component. Alternatively, j represents the total angular momentum of the relative motion in the quark–antiquark system which describes the meson. The quantum numbers ℓ, s and n stand, respectively, for the orbital angular momentum, the spin, and the radial excitation of the constituents of the meson. Finally, $\mathcal{M}$ represents the 3×3 flavour matrix which indicates the valences of the quark and the antiquark.

Here, we study the decay intensities for the following processes:

$$\begin{aligned} &\text{meson}\,(J, J_z, \ell, s, n, \mathcal{M}_C) \\ &\quad\longrightarrow \text{meson}\,(j_1, M_1, \ell_1, s_1, n_1, \mathcal{M}_A) \\ &\qquad +\text{meson}\,(j_2, M_2, \ell_2, s_2, n_2, \mathcal{M}_B)\,. \end{aligned} \tag{10}$$

This is not a completely satisfactory notation, since the spin-z components M_1 and M_2 of the decay products in (10) are not supposed to be observable and, moreover, the quantum numbers which characterise the relative motion of the decay products are not specified in (10), despite being equally important. Let us indicate the orbital quantum numbers of the two-meson system by means of an index, r, and hence denote the orbital angular momentum of the two mesons by ℓ_r, the total spin by s_r, and the radial excitation of the relative motion in the two-meson system by

$$\langle J, J_z, j_1, \ell_1, s_1, n_1, j_2, \ell_2, s_2, n_2, \ell_r, s_r, n_r, A, B\,|J, J_z, \ell, s, n, C\rangle$$
$$= \mathrm{Tr}\left\{\mathcal{M}_A\mathcal{M}_B{\mathcal{M}_C}^T\langle J, J_z, j_1, \ell_1, s_1, n_1, j_2, \ell_2, s_2, n_2, \ell_r, s_r, n_r\,|J, J_z, \ell, s, n, \boldsymbol{\alpha}_{ABC}\rangle\right.$$
$$\left.+\mathcal{M}_B\mathcal{M}_A{\mathcal{M}_C}^T\langle J, J_z, j_1, \ell_1, s_1, n_1, j_2, \ell_2, s_2, n_2, \ell_r, s_r, n_r\,|J, J_z, \ell, s, n, \boldsymbol{\alpha}_{BAC}\rangle\right\}. \quad (11)$$

Table 1. Particle identification used in this paper

symbol	multiplet
t	isotriplets
d	isodoublets
8	isoscalar SU_3 octet members
1	SU_3 singlets

n_r. The total angular momentum of the two-meson system and its z component are, due to angular-momentum conservation, given by J and J_z, respectively.

The decay probability for the process (10) is then, following the formalism developed in [21], given by the following matrix element: (see (11) on top of the page). The spatial parts in each of the two terms of the transition element (11) are denoted by

$$\langle J, J_z, j_1, \ell_1, s_1, n_1, j_2, \ell_2, s_2, n_2, \ell_r, s_r, n_r\,|J, J_z, \ell, s, n, \boldsymbol{\alpha}\rangle, \quad (12)$$

and are defined and explained in Appendix A. Notice that expression (11) manifestly preserves charge conjugation and G parity.

Since for many purposes it is sufficient to have flavour-independent coupling constants for the corresponding strong decay channels of pseudoscalar, vector, and scalar mesons, we tabulate the probabilities for the three-meson vertices of those decay processes; for a pseudoscalar meson in Table 2, for a vector meson in Table 3, and for a scalar meson in Table 4. In order to maintain the tables as condensed as possible, we represent mesons by symbols and by their quantum numbers. Since we assume that isospin is indeed a perfect symmetry, we may represent all members of an isomultiplet by the same symbol, for which we just have chosen the letters and numbers t, d, 8 and 1, according to the identification given in Table 1. Now let us just analyse one horizontal line of one of the three tables, to make sure that the reader understands what the numbers represent. Let us take the fourth line of Table 2. In the first column we find four zeroes, representing the internal spatial quantum numbers j, ℓ, s, and n of the first decay product, M_1, which hence characterises a meson out of the lowest-lying ($n = 0$) pseudoscalar nonet. In the second column we find similarly that the second decay product, M_2, represents a meson out of the lowest-lying vector nonet. In the third column we find the quantum numbers for the relative motion of M_1 and M_2, i.e., P-wave ($\ell_r = 1$) with total spin one ($s_r = 1$) in the lowest radial excitation ($n_r = 0$). Since the table refers to the real or virtual decays of the lowest-lying pseudoscalar meson nonet ($J\ell sn = 0000$, indicated in the top of the table), the next four columns refer to its isotriplet member, which is the pion. We then find that the pion couples with a strength $(1/6)^{1/2}$ to the tt (isotriplet–isotriplet) channel, which, following Table 1 and the particle assignments discussed above to M_1 and M_2, i.e., pseudoscalar and vector, respectively, represents in this case the $\pi\rho$ channel. Following a similar reasoning, we find that the pion couples with a strength $(1/12)^{1/2}$ to KK^*. The total coupling of a pion to pseudoscalar–vector channels is given in the column under T by $(1/4)^{1/2}$, which is the square root of the quadratic sum of the two previous couplings, i.e., $(1/6 + 1/12)^{1/2}$.

The next set of coupling constants refer to the real or virtual (actually only virtual) decays of a kaon. We find $(1/8)^{1/2}$ to td, which represents both of the possibilities pseudoscalar (isotriplet) + vector (isodoublet), i.e., πK^*, and pseudoscalar (isodoublet) + vector (isotriplet), i.e., $K\rho$, each with half of the intensity that is given in the table, and therefore one has for the kaon the coupling constants $(1/16)^{1/2}$ to πK^* and $(1/16)^{1/2}$ to $K\rho$. Next, we find in the table that the kaon couples with $(1/8)^{1/2}$ to $d8$, which represents both of the possibilities, pseudoscalar (isodoublet) + vector (SU_3 octet isoscalar), i.e., K + some mixture of the ω and ϕ mesons, and pseudoscalar (SU_3 octet isoscalar) + vector (isodoublet), i.e., some mixture of η's + K^*, each with half of the intensity that is given in the table, and hence one extracts for the kaon the coupling constants $(1/16)^{1/2}$ to $K + (\omega, \phi)$ and $(1/16)^{1/2}$ to $(\eta, \eta') + K^*$. The kaon does not couple to the $d1$ channels in the pseudoscalar + vector case, which represents the channels with one isodoublet and one SU_3 singlet. The total coupling for the kaon to its pseudoscalar + vector decay channels sums up to $(1/4)^{1/2}$, as one verifies in the column under T. The next two sets of coupling constants refer similarly to the decay modes of the isoscalar partners, either SU_3 octet or SU_3 singlet, of the pseudoscalar nonet. Mixings can be done by hand as exemplified in Appendix B.

Notice that for the SU_3 octet members one has flavour symmetry for each horizontal line in the tables. This does not go through for the SU_3 singlet partners, with the exception of scalar-meson decay (Table 4), where all horizontal lines have the same total coupling in each subsection of the table. However, all columns under T sum up to 1, representing full flavour symmetry once all possible decay channels have been accounted for.

5 Results

The pole structures of the scattering matrices for P-wave meson–meson scattering, or equivalently, the radial spectra of heavy and light pseudoscalar and vector mesons, were studied in the, largely non-relativistic, coupled channel NUMM, published in [7], hereafter referred to as B83,

Table 2. Coupling constants for the decay processes of pseudoscalar mesons into meson pairs. The interpretation of the content of the table is explained in the text

			flavour channels and totals for $M(J\ell sn = 0000)$																		
			SU_3 octet members													SU_3 singlets				
spatial q-numbers			isotriplets					isodoublets				isoscalars									
M_1	M_2	rel.	(t)					(d)				(8)					(1)				
$j\ell sn$	$j\ell sn$	ℓsn	tt	dd	$t8$	$t1$	T	td	$d8$	$d1$	T	tt	dd	88	81	T	tt	dd	88	11	T
0000	0110	000	-	$\frac{1}{24}$	$\frac{1}{36}$	$\frac{1}{18}$	$\frac{1}{8}$	$\frac{1}{16}$	$\frac{1}{144}$	$\frac{1}{18}$	$\frac{1}{8}$	$\frac{1}{24}$	$\frac{1}{72}$	$\frac{1}{72}$	$\frac{1}{18}$	$\frac{1}{8}$	$\frac{1}{12}$	$\frac{1}{9}$	$\frac{1}{36}$	$\frac{1}{36}$	$\frac{1}{4}$
1010	1100	000	-	$\frac{1}{24}$	$\frac{1}{36}$	$\frac{1}{18}$	$\frac{1}{8}$	$\frac{1}{16}$	$\frac{1}{144}$	$\frac{1}{18}$	$\frac{1}{8}$	$\frac{1}{24}$	$\frac{1}{72}$	$\frac{1}{72}$	$\frac{1}{18}$	$\frac{1}{8}$	$\frac{1}{12}$	$\frac{1}{9}$	$\frac{1}{36}$	$\frac{1}{36}$	$\frac{1}{4}$
1010	1110	000	$\frac{1}{6}$	$\frac{1}{12}$	-	-	$\frac{1}{4}$	$\frac{1}{8}$	$\frac{1}{8}$	-	$\frac{1}{4}$	-	$\frac{1}{4}$	-	-	$\frac{1}{4}$	-	-	-	-	-
0000	1010	110	$\frac{1}{6}$	$\frac{1}{12}$	-	-	$\frac{1}{4}$	$\frac{1}{8}$	$\frac{1}{8}$	-	$\frac{1}{4}$	-	$\frac{1}{4}$	-	-	$\frac{1}{4}$	-	-	-	-	-
1010	1010	110	-	$\frac{1}{12}$	$\frac{1}{18}$	$\frac{1}{9}$	$\frac{1}{4}$	$\frac{1}{8}$	$\frac{1}{72}$	$\frac{1}{9}$	$\frac{1}{4}$	$\frac{1}{12}$	$\frac{1}{36}$	$\frac{1}{36}$	$\frac{1}{9}$	$\frac{1}{4}$	$\frac{1}{6}$	$\frac{2}{9}$	$\frac{1}{18}$	$\frac{1}{18}$	$\frac{1}{2}$

Table 3. Coupling constants for the decay processes of vector mesons into meson pairs. The interpretation of the content of the table is explained in the text

			flavour channels and totals for $M(J\ell sn = 1010)$																		
			SU_3 octet members													SU_3 singlets				
spatial q-numbers			isotriplets					isodoublets				isoscalars									
M_1	M_2	rel.	(t)					(d)				(8)					(1)				
$j\ell sn$	$j\ell sn$	ℓsn	tt	dd	$t8$	$t1$	T	td	$d8$	$d1$	T	tt	dd	88	81	T	tt	dd	88	11	T
0000	1100	010	-	$\frac{1}{72}$	$\frac{1}{108}$	$\frac{1}{54}$	$\frac{1}{24}$	$\frac{1}{48}$	$\frac{1}{432}$	$\frac{1}{54}$	$\frac{1}{24}$	$\frac{1}{72}$	$\frac{1}{216}$	$\frac{1}{216}$	$\frac{1}{54}$	$\frac{1}{24}$	$\frac{1}{36}$	$\frac{1}{27}$	$\frac{1}{108}$	$\frac{1}{108}$	$\frac{1}{12}$
0000	1110	010	$\frac{1}{18}$	$\frac{1}{36}$	-	-	$\frac{1}{12}$	$\frac{1}{24}$	$\frac{1}{24}$	-	$\frac{1}{12}$	-	$\frac{1}{12}$	-	-	$\frac{1}{12}$	-	-	-	-	-
1010	1100	010	$\frac{1}{18}$	$\frac{1}{36}$	-	-	$\frac{1}{12}$	$\frac{1}{24}$	$\frac{1}{24}$	-	$\frac{1}{12}$	-	$\frac{1}{12}$	-	-	$\frac{1}{12}$	-	-	-	-	-
1010	1110	010	-	$\frac{1}{18}$	$\frac{1}{27}$	$\frac{2}{27}$	$\frac{1}{6}$	$\frac{1}{12}$	$\frac{1}{108}$	$\frac{2}{27}$	$\frac{1}{6}$	$\frac{1}{18}$	$\frac{1}{54}$	$\frac{1}{54}$	$\frac{2}{27}$	$\frac{1}{6}$	$\frac{1}{9}$	$\frac{4}{27}$	$\frac{1}{27}$	$\frac{1}{27}$	$\frac{1}{3}$
0110	1010	010	-	$\frac{1}{24}$	$\frac{1}{36}$	$\frac{1}{18}$	$\frac{1}{8}$	$\frac{1}{16}$	$\frac{1}{144}$	$\frac{1}{18}$	$\frac{1}{8}$	$\frac{1}{24}$	$\frac{1}{72}$	$\frac{1}{72}$	$\frac{1}{18}$	$\frac{1}{8}$	$\frac{1}{12}$	$\frac{1}{9}$	$\frac{1}{36}$	$\frac{1}{36}$	$\frac{1}{4}$
0000	0000	100	$\frac{1}{36}$	$\frac{1}{72}$	-	-	$\frac{1}{24}$	$\frac{1}{48}$	$\frac{1}{48}$	-	$\frac{1}{24}$	-	$\frac{1}{24}$	-	-	$\frac{1}{24}$	-	-	-	-	-
1010	1010	100	$\frac{1}{108}$	$\frac{1}{216}$	-	-	$\frac{1}{72}$	$\frac{1}{144}$	$\frac{1}{144}$	-	$\frac{1}{72}$	-	$\frac{1}{72}$	-	-	$\frac{1}{72}$	-	-	-	-	-
0000	1010	110	-	$\frac{1}{18}$	$\frac{1}{27}$	$\frac{2}{27}$	$\frac{1}{6}$	$\frac{1}{12}$	$\frac{1}{108}$	$\frac{2}{27}$	$\frac{1}{6}$	$\frac{1}{18}$	$\frac{1}{54}$	$\frac{1}{54}$	$\frac{2}{27}$	$\frac{1}{6}$	$\frac{1}{9}$	$\frac{4}{27}$	$\frac{1}{27}$	$\frac{1}{27}$	$\frac{1}{3}$
1010	1010	120	$\frac{5}{27}$	$\frac{5}{54}$	-	-	$\frac{5}{18}$	$\frac{5}{36}$	$\frac{5}{36}$	-	$\frac{5}{18}$	-	$\frac{5}{18}$	-	-	$\frac{5}{18}$	-	-	-	-	-

Table 4. Coupling constants for the decay processes of scalar mesons into meson pairs. The interpretation of the content of the table is explained in the text

			flavour channels and totals for $M(J\ell sn = 0110)$																		
			SU_3 octet members													SU_3 singlets				
spatial q-numbers			isotriplets					isodoublets				isoscalars									
M_1	M_2	rel.	(t)					(d)				(8)					(1)				
$j\ell sn$	$j\ell sn$	ℓsn	tt	dd	$t8$	$t1$	T	td	$d8$	$d1$	T	tt	dd	88	81	T	tt	dd	88	11	T
0000	0000	001	-	$\frac{1}{72}$	$\frac{1}{108}$	$\frac{1}{54}$	$\frac{1}{24}$	$\frac{1}{48}$	$\frac{1}{432}$	$\frac{1}{54}$	$\frac{1}{24}$	$\frac{1}{72}$	$\frac{1}{216}$	$\frac{1}{216}$	$\frac{1}{54}$	$\frac{1}{24}$	$\frac{1}{72}$	$\frac{1}{54}$	$\frac{1}{216}$	$\frac{1}{216}$	$\frac{1}{24}$
0000	0001	000	-	$\frac{1}{144}$	$\frac{1}{216}$	$\frac{1}{108}$	$\frac{1}{48}$	$\frac{1}{96}$	$\frac{1}{864}$	$\frac{1}{108}$	$\frac{1}{48}$	$\frac{1}{144}$	$\frac{1}{432}$	$\frac{1}{432}$	$\frac{1}{108}$	$\frac{1}{48}$	$\frac{1}{144}$	$\frac{1}{108}$	$\frac{1}{432}$	$\frac{1}{432}$	$\frac{1}{48}$
1010	1010	001	-	$\frac{1}{216}$	$\frac{1}{324}$	$\frac{1}{162}$	$\frac{1}{72}$	$\frac{1}{144}$	$\frac{1}{1296}$	$\frac{1}{162}$	$\frac{1}{72}$	$\frac{1}{216}$	$\frac{1}{648}$	$\frac{1}{648}$	$\frac{1}{162}$	$\frac{1}{72}$	$\frac{1}{216}$	$\frac{1}{162}$	$\frac{1}{648}$	$\frac{1}{648}$	$\frac{1}{72}$
1010	1011	000	-	$\frac{1}{432}$	$\frac{1}{648}$	$\frac{1}{324}$	$\frac{1}{144}$	$\frac{1}{288}$	$\frac{1}{2592}$	$\frac{1}{324}$	$\frac{1}{144}$	$\frac{1}{432}$	$\frac{1}{1296}$	$\frac{1}{1296}$	$\frac{1}{324}$	$\frac{1}{144}$	$\frac{1}{432}$	$\frac{1}{324}$	$\frac{1}{1296}$	$\frac{1}{1296}$	$\frac{1}{144}$
1010	1210	000	-	$\frac{5}{108}$	$\frac{5}{162}$	$\frac{5}{81}$	$\frac{5}{36}$	$\frac{5}{72}$	$\frac{5}{648}$	$\frac{5}{81}$	$\frac{5}{36}$	$\frac{5}{108}$	$\frac{5}{324}$	$\frac{5}{324}$	$\frac{5}{81}$	$\frac{5}{36}$	$\frac{5}{108}$	$\frac{5}{81}$	$\frac{5}{324}$	$\frac{5}{324}$	$\frac{5}{36}$
1100	1100	000	-	$\frac{1}{144}$	$\frac{1}{216}$	$\frac{1}{108}$	$\frac{1}{48}$	$\frac{1}{96}$	$\frac{1}{864}$	$\frac{1}{108}$	$\frac{1}{48}$	$\frac{1}{144}$	$\frac{1}{432}$	$\frac{1}{432}$	$\frac{1}{108}$	$\frac{1}{48}$	$\frac{1}{144}$	$\frac{1}{108}$	$\frac{1}{432}$	$\frac{1}{432}$	$\frac{1}{48}$
0110	0110	000	-	$\frac{1}{48}$	$\frac{1}{72}$	$\frac{1}{36}$	$\frac{1}{16}$	$\frac{1}{32}$	$\frac{1}{288}$	$\frac{1}{36}$	$\frac{1}{16}$	$\frac{1}{48}$	$\frac{1}{144}$	$\frac{1}{144}$	$\frac{1}{36}$	$\frac{1}{16}$	$\frac{1}{48}$	$\frac{1}{36}$	$\frac{1}{144}$	$\frac{1}{144}$	$\frac{1}{16}$
1110	1110	000	-	$\frac{1}{36}$	$\frac{1}{54}$	$\frac{1}{27}$	$\frac{1}{12}$	$\frac{1}{24}$	$\frac{1}{216}$	$\frac{1}{27}$	$\frac{1}{12}$	$\frac{1}{36}$	$\frac{1}{108}$	$\frac{1}{108}$	$\frac{1}{27}$	$\frac{1}{12}$	$\frac{1}{36}$	$\frac{1}{27}$	$\frac{1}{108}$	$\frac{1}{108}$	$\frac{1}{12}$
0000	1110	110	-	$\frac{1}{18}$	$\frac{1}{27}$	$\frac{2}{27}$	$\frac{1}{6}$	$\frac{1}{12}$	$\frac{1}{108}$	$\frac{2}{27}$	$\frac{1}{6}$	$\frac{1}{18}$	$\frac{1}{54}$	$\frac{1}{54}$	$\frac{2}{27}$	$\frac{1}{6}$	$\frac{1}{18}$	$\frac{2}{27}$	$\frac{1}{54}$	$\frac{1}{54}$	$\frac{1}{6}$
1010	1100	110	-	$\frac{1}{18}$	$\frac{1}{27}$	$\frac{2}{27}$	$\frac{1}{6}$	$\frac{1}{12}$	$\frac{1}{108}$	$\frac{2}{27}$	$\frac{1}{6}$	$\frac{1}{18}$	$\frac{1}{54}$	$\frac{1}{54}$	$\frac{2}{27}$	$\frac{1}{6}$	$\frac{1}{18}$	$\frac{2}{27}$	$\frac{1}{54}$	$\frac{1}{54}$	$\frac{1}{6}$
1010	1010	220	-	$\frac{5}{54}$	$\frac{5}{81}$	$\frac{10}{81}$	$\frac{5}{18}$	$\frac{5}{36}$	$\frac{5}{324}$	$\frac{10}{81}$	$\frac{5}{18}$	$\frac{5}{54}$	$\frac{5}{162}$	$\frac{5}{162}$	$\frac{10}{81}$	$\frac{5}{18}$	$\frac{5}{54}$	$\frac{10}{81}$	$\frac{5}{162}$	$\frac{5}{162}$	$\frac{5}{18}$

Table 5. Quadratic coupling constants for the decay process of a scalar meson into a pair of pseudoscalar mesons

initial meson	decay products	
	[11]	[23]
a_0 or δ	$\frac{1}{3}\ (K\bar{K})\ +\ \frac{2}{3}\ (\pi\eta_n)$	$\frac{1}{3}\ (K\bar{K})$ and $\frac{2}{3}$ (sum $\pi\eta$'s)
K_0^* or κ	$\frac{1}{2}\ (K\pi)\ +\ \frac{1}{2}\ (K\eta_n{+}K\eta_s)$	$\frac{1}{2}\ (K\pi)$ and $\frac{1}{2}$ (sum $K\eta$'s)
f_0 or $\epsilon/S\ n\bar{n}$	$\frac{3}{5}\ (\pi\pi)\ +\ \frac{1}{5}\ (K\bar{K})\ +\ \frac{1}{5}\ (\eta_n\eta_n)$	1 $(\pi\pi)$, $\frac{1}{3}\ (K\bar{K})$ and $\frac{1}{3}$ (sum $\eta\eta$'s)
f_0 or $\epsilon/S\ s\bar{s}$	$\frac{1}{2}\ (K\bar{K})\ +\ \frac{1}{2}\ (\eta_s\eta_s)$	$\frac{2}{3}\ (K\bar{K})$ and $\frac{2}{3}$ (sum $\eta\eta$'s)

in which the authors parametrised confinement by a universal frequency, the same for all flavours, including charm and bottom. The universal frequency and a flavour-independent overall coupling constant, representing the probability for the creation of a $^3P_0$ light quark–antiquark pair, were sufficient to obtain theoretical predictions for phase shifts and scattering cross sections, or equivalently, for central resonance positions and widths, which were in reasonable agreement with the data. All relative couplings were exactly taken as given in Tables 2 and 3, though some of these had been derived in a more empirical way, and were then extended in order to also include the heavy-quark systems. This extension is quite trivial and will not be discussed here. The only flavour non-invariance came from the quark masses and the two-meson thresholds, all other ingredients were the same for all flavours. Of course, many of the decay channels were omitted, assuming their thresholds to be high enough in energy, so as not to have too much importance for the details of the scattering processes at much lower energies. But this is only a practical ingredient, not to be confused with flavour breaking.

In [22], the electromagnetic transitions in the charmonium and bottomonium systems were studied, using the quark and meson distributions from B83, with good results, indicating that not only the pole structures of the scattering matrices, but also the related wave functions stood the confrontation with experiment.

In [11], hereafter referred to as B86, the pole structure of the scattering matrix was inspected for S-wave meson–meson scattering. Since the model was the same as for B83, using exactly the same universal frequency, flavour-independent overall coupling constant, and quark masses, the calculated phase shifts and scattering cross sections could be considered genuine theoretical predictions. The agreement with the data was unexpected, especially because it had not been the objective of the model, neither was the model constructed towards fitting the S-wave scattering data. All relative couplings were exactly taken as given in Table 4. Also here, only those two-meson channels were taken into account which contain members of the lowest-lying pseudoscalar and vector nonets. That such a procedure does not break flavour invariance may be explicitly verified by checking the first, third, and last line in Table 4.

The observed flavour independence of the strong interactions is a very important ingredient for low-energy hadron physics and is woven into the NUMM; first, by the universal frequency, which makes the ratio of the kinetic term and the potential term of the model flavour independent and hence also the level splittings; second, by the intensities of the three-meson vertices for the coupling to the various decay channels.

6 Comparison of two models

As stated in the Introduction, it is not easy to compare meson models, but here we will pay attention to the comparison of the NUMM with a model [23], hereafter referred to as T95, which is tailor-made for scalar mesons or, in other words, for S-wave meson–meson scattering. The latter model, a revised version of the HUQM, was confronted with experiment in an analysis published in [24], hereafter referred to as TR96. Based on the good agreement of its theoretical predictions with the available experimental phase shifts, one may be inclined to accept all further conclusions presented in the same publication, such as the existence and location of resonances. However, the authors failed to find the complex-energy pole corresponding to the established $f_0(1500)$ resonance. Furthermore, they also did not find a light K_0^*, i.e., the old κ, somewhere between 700 and 1100 MeV. Although the latter resonance is not (yet) established experimentally, it has recently received renewed phenomenological and theoretical support [25–27] (see also [28]). Moreover, its absence from nature would imply a breaking of the conventional nonet pattern for mesons. On the other hand, if a light K_0^* is confirmed, then there exist unmistakable experimental candidates for *two complete* scalar nonets, as predicted by B86. So it is intriguing to figure out why model T95/TR96, which is very similar in its philosophy and also in observing a resonance doubling, at least for some states, does not reproduce this resonance.

In Table 5, we collect the intensities for strong scalar-meson decay into a pair of pseudoscalar mesons, under the assumption that pions, kaons and etas have equal masses, as given by models B86 and T95/TR96. For the purpose of comparison, we have multiplied the values given in B86 by a constant factor. The resulting values can also be read from the first line of Table 4 when renormalised (i.e., multiplied by a factor 24), and when isoscalar mixing has been dealt with as outlined in Appendix B. Now notice that, by

using (5), the total decay intensities stemming from [11] become equal to A for all scalar mesons, as demanded by flavour blindness, i.e.,

$$\Gamma(a_0) = \Gamma(\kappa) = \Gamma(f_0, n\bar{n}) = \Gamma(f_0, s\bar{s}) = A. \quad (13)$$

For model T95/TR96, the comparable intensities are derived from a point-particle approach to the three-meson vertex, which results in coupling constants given by

$$\lambda \mathrm{Tr}\left(\mathcal{M}_A\mathcal{M}_B\mathcal{M}_C \pm \mathcal{M}_B\mathcal{M}_A\mathcal{M}_C\right), \quad (14)$$

where A, B and C stand for the three mesons involved at the vertex $C \to AB$, and $\mathcal{M}_X$ is the 3×3 flavour matrix for meson X. It is understood in (14) that either the symmetric or the antisymmetric trace is to be taken, depending on the sign of the product of the three charge-conjugation quantum numbers. In this way, charge conjugation and G parity are automatically preserved.

Flavour symmetry as from (14), and using formula (5), yields in this case the flavour-dependent result

$$\Gamma(a_0) = \Gamma(\kappa) = \frac{3}{5}\Gamma(f_0, n\bar{n}) = \frac{3}{4}\Gamma(f_0, s\bar{s}) = A, \quad (15)$$

in contrast with the results shown in (13).

The reason for this discrepancy can be explained as follows. The vertex (14) is $SU(3)_{\mathrm{flavour}}$ symmetric. This does, however, not imply flavour blindness, since the strengths for $SU(3)_{\mathrm{flavour}}$-octet meson decays may (and do here!) differ from the strengths of the $SU(3)_{\mathrm{flavour}}$-singlet meson decays. Moreover, the coupling constant λ of the vertex (14) only applies to the specific case of the scalar to two pseudoscalar mesons. For other vertices, other couplings have to be chosen and adjusted to the data.

In our appraoch, all three-meson vertices are related, since they all follow from (11), and therefore make it possible to define the universal coupling constant that is one of the cornerstones of model B83. Moreover, flavour blindness is guaranteed. In order to see this for the specific decays under discussion here, let us have a closer look at the normalisation factor which we find in (16) of Appendix (A). This factor stems from the initial four-particle wave function of the two $q\bar{q}$ pairs. Now, for the $SU(3)_{\mathrm{flavour}}$-singlet lowest-lying ($n = 0$) scalar ($J^{PC} = 0^{++}$) mesons, both pairs have the same quantum numbers in the $^3P_0$ model, and hence a non-trivial wave-function normalisation, leading to the result (13).

It appears to be due to the flavour dependence of (15), in the sense which we explained above, that the authors of TR96, which based their calculations on the coupling constants from T95, did not observe any resonance doubling for the isodoublet and one of the two isoscalars, and therefore miss the $K_0^*(700\text{-}1100)$ and $f_0(1500)$ poles needed to complete two scalar-meson nonets.

The normalisation factors that are relevant to (13) are given in (16) and (17) of Appendix A. In Appendix B, we show how they lead exactly to the factors 3/5 and 3/4 which are necessary to compensate the flavour dependence of (15).

A Rearrangement coefficients

The spatial parts of the matrix elements (11) are, following the formalism developed in [21], in the approximation of equal flavour masses just given by Clebsch–Gordonary and some overlap integrals, amounting to

$$\left.\begin{matrix}\langle J, J_z, j_1, \ell_1, s_1, n_1, j_2, \ell_2, s_2, n_2, \ell_r, s_r, n_r \,|J, J_z, \ell, s, n, \boldsymbol{\alpha}_{ABC}\rangle \\ \langle J, J_z, j_1, \ell_1, s_1, n_1, j_2, \ell_2, s_2, n_2, \ell_r, s_r, n_r \,|J, J_z, \ell, s, n, \boldsymbol{\alpha}_{BAC}\rangle\end{matrix}\right\}$$
$$= \frac{1}{\sqrt{1 + \langle C\,|SU(3)_{\mathrm{flavour}}\text{-singlet}\rangle\delta(^{2s+1}\ell_J, ^3P_0)\delta_{n0}}}$$
$$\times \sum_{\{\mu\},\{m\},\{M\}} \begin{pmatrix} s_r & \ell_r & J \\ M_r & m_r & J_z\end{pmatrix}\begin{pmatrix} j_1 & j_2 & s_r \\ M_1 & M_2 & M_r\end{pmatrix}\begin{pmatrix} \ell_1 & s_1 & j_1 \\ m_1 & \mu_1 & M_1\end{pmatrix}$$
$$\times \begin{pmatrix} \ell_2 & s_2 & j_2 \\ m_2 & \mu_2 & M_2\end{pmatrix}\begin{pmatrix} \ell & s & J \\ m_\ell & \mu_s & J_z\end{pmatrix}\begin{pmatrix} 1 & 1 & 0 \\ m & -m & 0\end{pmatrix}\begin{pmatrix} \frac{1}{2} & \frac{1}{2} & s_1 \\ \mu_a & \mu_b & \mu_1\end{pmatrix}$$
$$\times \begin{pmatrix} \frac{1}{2} & \frac{1}{2} & s_2 \\ \mu_c & \mu_d & \mu_2\end{pmatrix}$$
$$\times \left\{\begin{matrix}\begin{pmatrix} \frac{1}{2} & \frac{1}{2} & s \\ \mu_a & \mu_d & \mu_s\end{pmatrix}\begin{pmatrix} \frac{1}{2} & \frac{1}{2} & 1 \\ \mu_c & \mu_b & -m\end{pmatrix}\begin{pmatrix} n & \ell & m_\ell & n_1 & \ell_1 & m_1 \\ 0 & 1 & m & n_2 & \ell_2 & m_2 \\ 0 & 0 & 0 & n_r & \ell_r & m_r\end{pmatrix}_{\boldsymbol{\alpha}_{ABC}} \\ \begin{pmatrix} \frac{1}{2} & \frac{1}{2} & s \\ \mu_c & \mu_b & \mu_s\end{pmatrix}\begin{pmatrix} \frac{1}{2} & \frac{1}{2} & 1 \\ \mu_a & \mu_d & -m\end{pmatrix}\begin{pmatrix} n & \ell & m_\ell & n_1 & \ell_1 & m_1 \\ 0 & 1 & m & n_2 & \ell_2 & m_2 \\ 0 & 0 & 0 & n_r & \ell_r & m_r\end{pmatrix}_{\boldsymbol{\alpha}_{BAC}}\end{matrix}\right. , \quad (16)$$

where the sum is over all μ's, m's, and M's that appear in the formula, and where

$$\begin{aligned}&\langle C\,|SU(3)_{\mathrm{flavour}}\text{-singlet}\rangle \\ &= 0 \quad \text{for} \quad |C\rangle \quad \text{orthogonal to the} \\ &\qquad\qquad SU(3)_{\mathrm{flavour}}\text{-singlet state}, \\ &\quad \tfrac{1}{3} \quad \text{for} \quad |C\rangle = |u\bar{u}\rangle, \big|d\bar{d}\big\rangle, \quad \text{or} \quad |s\bar{s}\rangle, \\ &\quad \tfrac{2}{3} \quad \text{for} \quad |C\rangle = \sqrt{\tfrac{1}{2}}\left\{|u\bar{u}\rangle + \big|d\bar{d}\big\rangle\right\}, \\ &\quad 1 \quad \text{for} \quad |C\rangle = \sqrt{\tfrac{1}{3}}\left\{|u\bar{u}\rangle + \big|d\bar{d}\big\rangle + |s\bar{s}\rangle\right\}, \end{aligned} \quad (17)$$

and where

$$\delta(^{2s+1}\ell_J, ^3P_0) = \delta_{J0}\delta_{\ell1}\delta_{s1}. \quad (18)$$

The central part of (16) is constituted by the rearrangement coefficients, which can be given by the following diagrammatic representation

$$
\begin{aligned}
&\begin{pmatrix} n\ \ell\ m_\ell & n_1\ \ell_1\ m_1 \\ 0\ 1\ m & n_2\ \ell_2\ m_2 \\ 0\ 0\ 0 & n_r\ \ell_r\ m_r \end{pmatrix}_{\boldsymbol{\alpha}} \\
&= (-1)^{n+n_1+n_2+n_r} \left(\frac{\pi}{4}\right)^3 \sqrt{(n!n_1!n_2!n_r!)} \\
&\times \sqrt{\left(\frac{\Gamma\left(2n+\ell+\frac{3}{2}\right)\Gamma\left(\frac{5}{2}\right)\Gamma\left(\frac{3}{2}\right)\Gamma\left(2n_1+\ell_1+\frac{3}{2}\right)\Gamma\left(2n_2+\ell_2+\frac{3}{2}\right)\Gamma\left(2n_r+\ell_r+\frac{3}{2}\right)}{(2\ell+1)\,(3)\,(2\ell_1+1)\,(2\ell_2+1)\,(2\ell_r+1)} \right)} \\
&\times \sum_{\{n_{ij},\ell_{ij},m_{ij}\}} \prod_{i,j} (\alpha_{ij})^{2n_{ij}+\ell_{ij}} \frac{(2\ell_{ij}+1)}{n_{ij}!\Gamma\left(n_{ij}+\ell_{ij}+\frac{3}{2}\right)} \delta\left(2\left[n_{11}+n_{21}+n_{31}\right]+\ell_{11}+\ell_{21}+\ell_{31}, 2n+\ell\right) \\
&\times\delta\left(2\left[n_{12}+n_{22}+n_{32}\right]+\ell_{12}+\ell_{22}+\ell_{32}, 1\right)\delta\left(2\left[n_{13}+n_{23}+n_{33}\right]+\ell_{13}+\ell_{23}+\ell_{33}, 0\right) \\
&\times\delta\left(2\left[n_{11}+n_{12}+n_{13}\right]+\ell_{11}+\ell_{12}+\ell_{13}, 2n_1+\ell_1\right)\delta\left(2\left[n_{21}+n_{22}+n_{23}\right]+\ell_{21}+\ell_{22}+\ell_{23}, 2n_2+\ell_2\right) \\
&\times\delta\left(2\left[n_{31}+n_{32}+n_{33}\right]+\ell_{31}+\ell_{32}+\ell_{33}, 2n_r+\ell_r\right) \\
&\times \left(\begin{array}{ccc|c} \ell_{11} & \ell_{21} & \ell_{31} & \ell \\ m_{11} & m_{21} & m_{31} & m_\ell \end{array}\right) \left(\begin{array}{ccc|c} \ell_{12} & \ell_{22} & \ell_{32} & 1 \\ m_{12} & m_{22} & m_{32} & m \end{array}\right) \left(\begin{array}{ccc|c} \ell_{13} & \ell_{23} & \ell_{33} & 0 \\ m_{13} & m_{23} & m_{33} & 0 \end{array}\right) \\
&\times \left(\begin{array}{ccc|c} \ell_{11} & \ell_{12} & \ell_{13} & \ell_1 \\ m_{11} & m_{12} & m_{13} & m_1 \end{array}\right) \left(\begin{array}{ccc|c} \ell_{21} & \ell_{22} & \ell_{23} & \ell_2 \\ m_{21} & m_{22} & m_{23} & m_2 \end{array}\right) \left(\begin{array}{ccc|c} \ell_{31} & \ell_{32} & \ell_{33} & \ell_r \\ m_{31} & m_{32} & m_{33} & m_r \end{array}\right), \qquad (20)
\end{aligned}
$$

$$
\begin{pmatrix} n\ \ell\ m_\ell & n_1\ \ell_1\ m_1 \\ 0\ 1\ m & n_2\ \ell_2\ m_2 \\ 0\ 0\ 0 & n_r\ \ell_r\ m_r \end{pmatrix}_{\boldsymbol{\alpha}} = \qquad (19)
$$

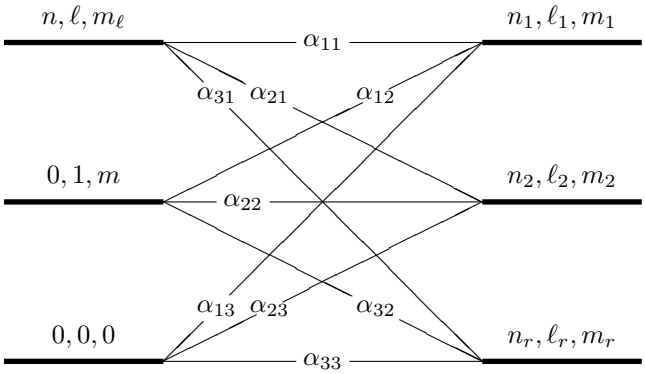

The upper-left external line carries the relevant quantum numbers of the initial meson in (10), the middle-left external line the quantum numbers of the $^3P_0$ $q\bar{q}$ pair, and the lower-left external line the quantum numbers of the relative motion of the two quark–antiquark systems, which, to lowest order, is supposed to be in its ground state. The external lines on the right-hand side of the diagram carry the quantum numbers of the decay products of (10) and their relative motion.

As explained in [20], each of the internal lines ij of the diagram in (19) carries the set of quantum numbers $\{n_{ij}, \ell_{ij}, m_{ij}\}$, over all possibilities of which must be summed, thereby respecting partial quantum-number conservation at each vertex, i.e., (see (20) on top of this page) where the angular-momenta recoupling coefficients are defined by

$$
\begin{aligned}
&\left(\begin{array}{ccc|c} \ell_1 & \ell_2 & \ell_3 & \ell \\ m_1 & m_2 & m_3 & m \end{array}\right) \\
&= \sum_{L,M} \begin{pmatrix} \ell_1 & \ell_2 & L \\ m_1 & m_2 & M \end{pmatrix} \begin{pmatrix} L & \ell_3 & \ell \\ M & m_3 & m \end{pmatrix} \begin{pmatrix} \ell_1 & \ell_2 & L \\ 0 & 0 & 0 \end{pmatrix} \begin{pmatrix} L & \ell_3 & \ell \\ 0 & 0 & 0 \end{pmatrix}, \qquad (21)
\end{aligned}
$$

and where the $\boldsymbol{\alpha}$ matrices, for the case of equal constituent flavour masses, are given by

$$
\boldsymbol{\alpha}_{ABC} = \begin{pmatrix} \frac{1}{2} & \frac{1}{2} & -\sqrt{\frac{1}{2}} \\ \frac{1}{2} & \frac{1}{2} & \sqrt{\frac{1}{2}} \\ -\sqrt{\frac{1}{2}} & \sqrt{\frac{1}{2}} & 0 \end{pmatrix} \qquad \text{and}
$$

$$
\boldsymbol{\alpha}_{BAC} = \begin{pmatrix} \frac{1}{2} & \frac{1}{2} & \sqrt{\frac{1}{2}} \\ \frac{1}{2} & \frac{1}{2} & -\sqrt{\frac{1}{2}} \\ \sqrt{\frac{1}{2}} & -\sqrt{\frac{1}{2}} & 0 \end{pmatrix}. \qquad (22)
$$

The allowed values for the quantum numbers of the internal lines of diagram (19), given by n_{ij} and ℓ_{ij} in (20), are non-negative integers and hence, because of partial quantum-number conservation at each vertex of the diagram, which is moreover expressed by the Kronecker deltas in (20), we find

$$
\begin{aligned}
&n_{12} = n_{22} = n_{32} = n_{13} = n_{23} = n_{33} = \ell_{13} = \ell_{23} \\
&\quad = \ell_{33} = 0, \qquad (23)
\end{aligned}
$$

which, also substituting the $\boldsymbol{\alpha}$ matrices (22), simplifies the expression for the rearrangement coefficients to (see (24)

$$
\begin{aligned}
&\begin{pmatrix} n\ \ell\ m_\ell & n_1\ \ell_1\ m_1 \\ 0\ 1\ m & n_2\ \ell_2\ m_2 \\ 0\ 0\ 0 & n_r\ \ell_r\ m_r \end{pmatrix} \left\{ \begin{matrix} \boldsymbol{\alpha}_{ABC} \\ \boldsymbol{\alpha}_{BAC} \end{matrix} \right\} \\
&= (-1)^{n+n_1+n_2+n_r} \left(\frac{\pi}{4}\right)^3 \sqrt{(n!n_1!n_2!n_r!)} \\
&\times \sqrt{\left(\frac{\Gamma\left(2n+\ell+\frac{3}{2}\right)\Gamma\left(\frac{5}{2}\right)\Gamma\left(\frac{3}{2}\right)\Gamma\left(2n_1+\ell_1+\frac{3}{2}\right)\Gamma\left(2n_2+\ell_2+\frac{3}{2}\right)\Gamma\left(2n_r+\ell_r+\frac{3}{2}\right)}{(2\ell+1)\,(3)\,(2\ell_1+1)\,(2\ell_2+1)\,(2\ell_r+1)} \right)} \\
&\times \left(\tfrac{1}{2}\right)^{2n+\ell+1-n_r-\frac{1}{2}\ell_r} \sum_{\{n_{ij},\ell_{ij},m_{ij}\}} \left\{ \begin{matrix} (-1)^{\ell_{31}} \\ \\ (-1)^{\ell_{32}} \end{matrix} \right\} \frac{1}{n_{11}!n_{21}!n_{31}!} \frac{(2\ell_{11}+1)\,(2\ell_{12}+1)}{\Gamma\left(n_{11}+\ell_{11}+\frac{3}{2}\right)\Gamma\left(\ell_{12}+\frac{3}{2}\right)\Gamma\left(\frac{3}{2}\right)} \\
&\times \frac{(2\ell_{21}+1)\,(2\ell_{22}+1)}{\Gamma\left(n_{21}+\ell_{21}+\frac{3}{2}\right)\Gamma\left(\ell_{22}+\frac{3}{2}\right)\Gamma\left(\frac{3}{2}\right)} \frac{(2\ell_{31}+1)\,(2\ell_{32}+1)}{\Gamma\left(n_{31}+\ell_{31}+\frac{3}{2}\right)\Gamma\left(\ell_{32}+\frac{3}{2}\right)\Gamma\left(\frac{3}{2}\right)} \delta\left(2\left[n_{11}+n_{21}+n_{31}\right]+\ell_{11}+\ell_{21}+\ell_{31}, 2n+\ell\right) \\
&\times \delta\left(\ell_{12}+\ell_{22}+\ell_{32}, 1\right) \delta\left(2n_{11}+\ell_{11}+\ell_{12}, 2n_1+\ell_1\right) \delta\left(2n_{21}+\ell_{21}+\ell_{22}, 2n_2+\ell_2\right) \delta\left(2n_{31}+\ell_{31}+\ell_{32}, 2n_r+\ell_r\right) \\
&\times \left(\begin{matrix} \ell_{11} & \ell_{21} & \ell_{31} \\ m_{11} & m_{21} & m_{31} \end{matrix} \middle| \begin{matrix} \ell \\ m_\ell \end{matrix} \right) \begin{pmatrix} \ell_{11} & \ell_{12} & \ell_1 \\ m_{11} & m_{12} & m_1 \end{pmatrix} \begin{pmatrix} \ell_{11} & \ell_{12} & \ell_1 \\ 0 & 0 & 0 \end{pmatrix} \begin{pmatrix} \ell_{21} & \ell_{22} & \ell_2 \\ m_{21} & m_{22} & m_2 \end{pmatrix} \begin{pmatrix} \ell_{21} & \ell_{22} & \ell_2 \\ 0 & 0 & 0 \end{pmatrix} \begin{pmatrix} \ell_{31} & \ell_{32} & \ell_r \\ m_{31} & m_{32} & m_r \end{pmatrix} \begin{pmatrix} \ell_{31} & \ell_{32} & \ell_r \\ 0 & 0 & 0 \end{pmatrix}. \qquad (24)
\end{aligned}
$$

on top of this page). Notice that the Kronecker deltas in (24) amount to

$$2n+\ell+1 = 2\left(n_1+n_2+n_r\right)+\ell_1+\ell_2+\ell_r, \qquad (25)$$

which is precisely the important relation that limits the number of possible decay channels.

Moreover, for an initial pseudoscalar or vector meson out of the lowest-lying flavour nonets, one has in (11) for the $q\bar{q}$ quantum numbers n and ℓ:

$$n = \ell = 0. \qquad (26)$$

Consequently, through the use of the Kronecker deltas in (24), we find for the quantum numbers of the internal lines of diagram (19) that

$$n_{11} = n_{21} = n_{31} = \ell_{11} = \ell_{21} = \ell_{31} = 0, \qquad (27)$$

and moreover

$$n_1 = n_2 = n_r = 0 \quad \text{and} \quad \ell_1+\ell_2+\ell_r = 1. \qquad (28)$$

Relations (28) can be checked against the first three colums of Tables 2 and 3, where for all possible channels the radial excitations n_1, n_2, or n_r vanish, and, moreover, the sums of ℓ_1, ℓ_2, and ℓ_r equal 1. This is a consequence of (25) and drastically limits the number of possible quantum numbers and hence decay channels.

For the relevant rearrangement coefficients we find, using (24), in this case

$$
\begin{aligned}
&\begin{pmatrix} 0\ 0\ 0 & 0\ \ell_1\ m_1 \\ 0\ 1\ m & 0\ \ell_2\ m_2 \\ 0\ 0\ 0 & 0\ \ell_r\ m_r \end{pmatrix} \left\{ \begin{matrix} \boldsymbol{\alpha}_{ABC} \\ \boldsymbol{\alpha}_{BAC} \end{matrix} \right\} \\
&= \left(\tfrac{1}{2}\right)^{1-\frac{1}{2}\ell_r} \left\{ \begin{matrix} +1 \\ \\ (-1)^{\ell_r} \end{matrix} \right\} \delta\left(\ell_1+\ell_2+\ell_r, 1\right). \qquad (29)
\end{aligned}
$$

For the decay of a meson out of the lowest-lying scalar nonet, one has

$$n = 0 \ \text{ and } \ell = s = 1, \qquad (30)$$

and hence, by the use of (24), one obtains for the relevant rearrangement coefficients in this case

$$
\begin{aligned}
&\begin{pmatrix} 0\ 1\ m_\ell & n_1\ \ell_1\ m_1 \\ 0\ 1\ m & n_2\ \ell_2\ m_2 \\ 0\ 0\ 0 & n_r\ \ell_r\ m_r \end{pmatrix} \left\{ \begin{matrix} \boldsymbol{\alpha}_{ABC} \\ \boldsymbol{\alpha}_{BAC} \end{matrix} \right\} \\
&= (-1)^{n_1+n_2+n_r} 8 \sqrt{(n_1!n_2!n_r!)} \\
&\times \sqrt{\left(\frac{\Gamma\left(2n_1+\ell_1+\frac{3}{2}\right)\Gamma\left(2n_2+\ell_2+\frac{3}{2}\right)\Gamma\left(2n_r+\ell_r+\frac{3}{2}\right)}{2\pi^{3/2}\,(2\ell_1+1)\,(2\ell_2+1)\,(2\ell_r+1)} \right)} \\
&\times \left(\tfrac{1}{2}\right)^{2n_1+2n_2+n_r+\ell_1+\ell_2+\frac{1}{2}\ell_r} \\
&\times \sum_{\{n_{ij},\ell_{ij},m_{ij}\}} \left\{ \begin{matrix} (-1)^{\ell_{31}} \\ \\ (-1)^{\ell_{32}} \end{matrix} \right\} \delta\left(\ell_{11}+\ell_{21}+\ell_{31}, 1\right) \\
&\times \delta\left(\ell_{12}+\ell_{22}+\ell_{32}, 1\right) \delta\left(\ell_{11}+\ell_{12}, 2n_1+\ell_1\right) \\
&\times \delta\left(\ell_{21}+\ell_{22}, 2n_2+\ell_2\right) \delta\left(\ell_{31}+\ell_{32}, 2n_r+\ell_r\right) \\
&\times \begin{pmatrix} \ell_{11} & \ell_{12} & \ell_1 \\ m_{11} & m_{12} & m_1 \end{pmatrix} \begin{pmatrix} \ell_{11} & \ell_{12} & \ell_1 \\ 0 & 0 & 0 \end{pmatrix} \begin{pmatrix} \ell_{21} & \ell_{22} & \ell_2 \\ m_{21} & m_{22} & m_2 \end{pmatrix} \\
&\times \begin{pmatrix} \ell_{21} & \ell_{22} & \ell_2 \\ 0 & 0 & 0 \end{pmatrix} \begin{pmatrix} \ell_{31} & \ell_{32} & \ell_r \\ m_{31} & m_{32} & m_r \end{pmatrix} \begin{pmatrix} \ell_{31} & \ell_{32} & \ell_r \\ 0 & 0 & 0 \end{pmatrix}. \qquad (31)
\end{aligned}
$$

B Mixing for scalar mesons

Since we assume $^3P_0$ quantum numbers for the creation of a $q\bar{q}$ pair out of the vacuum, the mixing of the isoscalar flavour-nonet members for lowest-lying scalar-meson decay is not completely trivial. So we will outline here some of the necessary ingredients.

In order to simplify the discussion, let us separate the normalisation factor and the summations in (16). Moreover, the two Kronecker deltas under the square root in formula (16) do not vanish for the lowest-lying scalar mesons. Therefore, let us denote

$$\left.\begin{array}{l}\langle 0,0,j_1,\ell_1,s_1,n_1,j_2,\ell_2,s_2,n_2,\ell_r,s_r,n_r\,|0,0,1,1,0,\boldsymbol{\alpha}_{ABC}\,\rangle \\ \\ \langle 0,0,j_1,\ell_1,s_1,n_1,j_2,\ell_2,s_2,n_2,\ell_r,s_r,n_r\,|0,0,1,1,0,\boldsymbol{\alpha}_{BAC}\,\rangle\end{array}\right\} = \frac{1}{\sqrt{1+\langle C\,|SU(3)_{\text{flavour}}\text{-singlet}\,\rangle}}\times\left\{\begin{array}{l}\langle ABC\rangle \\ \\ \langle BAC\rangle\end{array}\right. , \quad (32)$$

where $\langle ABC\rangle$ stands for the upper summation in (16) and $\langle BAC\rangle$ for the lower.

As one notices from (16), (19) and (20) or just only from (31), the transition coefficients $\langle ABC\rangle$ and $\langle BAC\rangle$ do not, for full flavour symmetry, i.e., for equal up, down and strange quark masses, depend on the flavour contents of the three mesons A, B, and C involved in the transition process (10), but just on the orbital and intrinsic spin quantum numbers of the system, which circumstance is also expressed by the notation of (12). In fact, for the case of equal quark masses, these transition coefficients are equal for each different set of spatial quantum numbers, up to a sign. This sign is positive for all possible couplings in the case of the lowest-lying scalar mesons. Consequently, since for Table 5 only the transitions between scalar mesons and pairs of pseudoscalar mesons are relevant, and for mixing in general only the restriction to a specific set of spatial quantum numbers has to be considered, we may here put

$$\langle ABC\rangle = \langle BAC\rangle. \quad (33)$$

For the transitions of the flavour-octet members to pairs of mesons, one has, according to (17), a unity normalisation factor. Let us study then the matrix elements for a representant, $u\bar{d}$, of the isotriplets, which is denoted by t in Table 4, coupled to an isoscalar, ϕ, and an isotriplet, for which we also take as a representant the $u\bar{d}$ state, and which, moreover, is also denoted by t in Table 4, i.e.,

$$\big\langle\big(u\bar{d}\big)\,\phi\,\big|u\bar{d}\big\rangle. \quad (34)$$

If ϕ represents the flavour-octet-member isoscalar ϕ_8, we find

$$\big\langle\big(u\bar{d}\big)\,\phi_8\,\big|u\bar{d}\big\rangle = \Big\langle\big(u\bar{d}\big)\,\sqrt{\tfrac{1}{6}}\,\big(u\bar{u}+d\bar{d}-2s\bar{s}\big)\,\big|u\bar{d}\Big\rangle.$$

Obviously, the matrix element for the $s\bar{s}$ contribution to ϕ_8 vanishes, hence

$$\big\langle\big(u\bar{d}\big)\,\phi_8\,\big|u\bar{d}\big\rangle = \sqrt{\tfrac{1}{6}}\,\big\{\big\langle\big(u\bar{d}\big)\,(u\bar{u})\,\big|u\bar{d}\big\rangle + \big\langle\big(u\bar{d}\big)\,\big(d\bar{d}\big)\,\big|u\bar{d}\big\rangle\big\}\,,$$

which, also using (33), gives

$$\begin{aligned}\big\langle\big(u\bar{d}\big)\,\phi_8\,\big|u\bar{d}\big\rangle &= \sqrt{\tfrac{1}{6}}\,\{\langle BAC\rangle + \langle ABC\rangle\} \\ &= \sqrt{\tfrac{2}{3}}\langle ABC\rangle. \end{aligned} \quad (35)$$

Following a similar reasoning when ϕ in (34) represents the flavour-singlet isoscalar ϕ_1, we find for its matrix elements the result

$$\begin{aligned}\big\langle\big(u\bar{d}\big)\,\phi_1\,\big|u\bar{d}\big\rangle &= \Big\langle\big(u\bar{d}\big)\,\sqrt{\tfrac{1}{3}}\,\big(u\bar{u}+d\bar{d}+s\bar{s}\big)\,\big|u\bar{d}\Big\rangle \\ &= \sqrt{\tfrac{4}{3}}\langle ABC\rangle. \end{aligned} \quad (36)$$

In Table 4, for the quadratic matrix elements under $t8$ and $t1$ in the sector *isotriplets*, one may verify the factor 2 that follows from (35) and (36).

For the ideally mixed isoscalars, ϕ_n (non-strange) and ϕ_s (strange) defined by

$$\begin{aligned}&\phi_n = \sqrt{\tfrac{1}{2}}\,\big(u\bar{u}+d\bar{d}\big) = \sqrt{\tfrac{2}{3}}\phi_1 + \sqrt{\tfrac{1}{3}}\phi_8 \ \text{ and} \\ &\phi_s = s\bar{s} = \sqrt{\tfrac{1}{3}}\phi_1 - \sqrt{\tfrac{2}{3}}\phi_8, \end{aligned} \quad (37)$$

one finds the matrix elements

$$\begin{aligned}\big\langle\big(u\bar{d}\big)\,\phi_n\,\big|u\bar{d}\big\rangle &= \sqrt{2}\langle ABC\rangle = \sqrt{3}\big\langle\big(u\bar{d}\big)\,\phi_8\,\big|u\bar{d}\big\rangle \\ &= \sqrt{\tfrac{3}{2}}\big\langle\big(u\bar{d}\big)\,\phi_1\,\big|u\bar{d}\big\rangle \ \text{ and} \\ \big\langle\big(u\bar{d}\big)\,\phi_s\,\big|u\bar{d}\big\rangle &= 0. \end{aligned} \quad (38)$$

Besides the multiplicative factor of 24 which is discussed in Sect. 6, (38) establishes the relation between the values given in the first line of Table 4 and the values given in Table 5 for the following matrix elements:

$$\begin{aligned}&\langle\pi\eta_n\,|a_0\,\rangle = \sqrt{24}\sqrt{3}\langle t8\,|t\,\rangle = \sqrt{\tfrac{2}{3}} \ \text{ and} \\ &\langle\pi\eta_s\,|a_0\,\rangle = 0. \end{aligned} \quad (39)$$

For the coupling of an isodoublet lowest-lying scalar meson to the isodoublet–isoscalar pair, we may also select representants. Let us consider the matrix element

$$\langle(u\bar{s})\,\phi\,|u\bar{s}\rangle.$$

In this case, the matrix element for the $d\bar{d}$ contribution vanishes. Consequently, for the isoscalar flavour singlets and octets, we end up with

$$\begin{aligned}&\langle(u\bar{s})\,\phi_1\,|u\bar{s}\rangle = \sqrt{\tfrac{4}{3}}\langle ABC\rangle \ \text{ and} \\ &\langle(u\bar{s})\,\phi_8\,|u\bar{s}\rangle = -\sqrt{\tfrac{1}{6}}\langle ABC\rangle, \end{aligned} \quad (40)$$

which explains the factor 8 in Table 4 for the quadratic matrix elements under $d8$ and $d1$, in the sector under *isodoublets*.

From (40), we obtain for the ideally mixed combinations (37) the relations

$$\langle(u\bar{s})\,\phi_n\,|u\bar{s}\rangle = \sqrt{\tfrac{1}{2}}\langle BAC\rangle = \sqrt{\tfrac{3}{8}}\langle(u\bar{s})\,\phi_1\,|u\bar{s}\rangle \quad \text{and}$$

$$\langle(u\bar{s})\,\phi_s\,|u\bar{s}\rangle = \langle ABC\rangle = \sqrt{\tfrac{3}{4}}\langle(u\bar{s})\,\phi_1\,|u\bar{s}\rangle,$$

which, by the use of the first line of Table 4 and when, moreover, multiplied by the factor $(24)^{1/2}$, gives the matrix elements of $\kappa \to K\eta_n$ and $\kappa \to K\eta_s$, i.e.,

$$\langle K\eta_n\,|\kappa\rangle = \sqrt{24}\sqrt{\tfrac{3}{8}}\langle d1\,|d\rangle = \sqrt{\tfrac{1}{6}} \quad \text{and}$$
$$\langle K\eta_s\,|\kappa\rangle = \sqrt{24}\sqrt{\tfrac{3}{4}}\langle d1\,|d\rangle = \sqrt{\tfrac{1}{3}},$$

the quadratic sum $(= \dfrac{1}{2})$ of which is found for model B86 in Table 5.

Now, according to (17), for the couplings of lowest-lying scalar isoscalars to meson pairs, the normalisation may be not unity. Let us begin with the coupling to a pair of isotriplets, e.g.

$$\big\langle\big(u\bar{d}\big)\,(d\bar{u})\,|\phi\big\rangle.$$

When ϕ represents a flavour-singlet isoscalar, then, also using (17) and (33), one finds

$$\begin{aligned}\big\langle\big(u\bar{d}\big)\,(d\bar{u})\,|\phi_1\big\rangle &= \Big\langle\big(u\bar{d}\big)\,(d\bar{u})\,\Big|\sqrt{\tfrac{1}{3}}\,\big(u\bar{u}+d\bar{d}+s\bar{s}\big)\Big\rangle \\ &= \sqrt{\tfrac{1}{3}}\left\{\frac{\langle ABC\rangle}{\sqrt{2}}+\frac{\langle BAC\rangle}{\sqrt{2}}\right\} \\ &= \sqrt{\tfrac{2}{3}}\langle ABC\rangle,\end{aligned}$$

whereas, when ϕ represents a flavour-octet isoscalar, it follows that

$$\big\langle\big(u\bar{d}\big)\,(d\bar{u})\,|\phi_8\big\rangle = \sqrt{\tfrac{1}{6}}\,\{\langle ABC\rangle + \langle BAC\rangle\} = \sqrt{\tfrac{2}{3}}\langle ABC\rangle.$$

Indeed, in Table 4 the quadratic matrix elements under tt in the sector for the flavour-octet isoscalars are the same as in the sector for the flavour-singlet isoscalars.

For the ideally mixed combination (37), also applying formulae (17) and (33), one obtains

$$\begin{aligned}\big\langle\big(u\bar{d}\big)\,(d\bar{u})\,|\phi_n\big\rangle &= \sqrt{\tfrac{1}{2}}\left\{\frac{\langle ABC\rangle}{\sqrt{\frac{5}{3}}}+\frac{\langle BAC\rangle}{\sqrt{\frac{5}{3}}}\right\} \\ &= \sqrt{\tfrac{6}{5}}\langle ABC\rangle = \sqrt{\tfrac{9}{5}}\big\langle\big(u\bar{d}\big)\,(d\bar{u})\,|\phi_1\big\rangle. \quad (41)\end{aligned}$$

When, moreover, multiplied by the factor $(24)^{1/2}$, (41) establishes the relation between the first line of Table 4 and the matrix element of $\eta_n \to \pi\pi$, according to

$$\langle\pi\pi\,|\eta_n\rangle = \sqrt{24}\sqrt{\tfrac{9}{5}}\langle tt\,|\phi_1\rangle = \sqrt{\tfrac{3}{5}},$$

as is found for model B86 in Table 5.

Next, let us also study the coupling of isoscalars to a pair of isodoublets, e.g.

$$\langle(u\bar{s})\,(s\bar{u})\,|\phi\rangle.$$

When ϕ represents a flavour-singlet isoscalar, then, again through the use of (17) and (33), we have

$$\begin{aligned}\langle(u\bar{s})\,(s\bar{u})\,|\phi_1\rangle &= \sqrt{\tfrac{1}{3}}\left\{\frac{\langle ABC\rangle}{\sqrt{2}}+\frac{\langle BAC\rangle}{\sqrt{2}}\right\} \\ &= \sqrt{\tfrac{2}{3}}\langle ABC\rangle. \quad (42)\end{aligned}$$

Similarly, for a flavour-octet isoscalar we find

$$\begin{aligned}\langle(u\bar{s})\,(s\bar{u})\,|\phi_8\rangle &= \sqrt{\tfrac{1}{6}}\,\{\langle ABC\rangle - 2\langle BAC\rangle\} \\ &= -\sqrt{\tfrac{1}{6}}\langle ABC\rangle, \quad (43)\end{aligned}$$

which result explains the factor 1/4 in Table 4 between the quadratic matrix elements under dd in the sectors for the flavour-octet isoscalars and for the flavour-singlet isoscalars.

For the ideally mixed isoscalars defined in (37), using once again (17), we obtain

$$\begin{aligned}\langle(u\bar{s})\,(s\bar{u})\,|\phi_n\rangle &= \sqrt{\tfrac{1}{2}}\frac{\langle ABC\rangle}{\sqrt{\frac{5}{3}}} = \sqrt{\tfrac{3}{10}}\langle ABC\rangle \\ &= \sqrt{\tfrac{9}{20}}\langle(u\bar{s})\,(s\bar{u})\,|\phi_1\rangle \quad \text{and}\end{aligned}$$

$$\begin{aligned}\langle(u\bar{s})\,(s\bar{u})\,|\phi_s\rangle &= \sqrt{\tfrac{1}{2}}\frac{\langle BAC\rangle}{\sqrt{\frac{4}{3}}} = \sqrt{\tfrac{3}{4}}\langle ABC\rangle \\ &= \sqrt{\tfrac{9}{8}}\langle(u\bar{s})\,(s\bar{u})\,|\phi_1\rangle,\end{aligned}$$

which nicely explains the values for the matrix elements of $(\eta_n/\eta_s) \to K\bar{K}$, i.e.,

$$\big\langle K\bar{K}\,|\eta_n\big\rangle = \sqrt{24}\sqrt{\tfrac{9}{20}}\langle dd\,|\phi_1\rangle = \sqrt{\tfrac{1}{5}} \quad \text{and}$$
$$\big\langle K\bar{K}\,|\eta_s\big\rangle = \sqrt{24}\sqrt{\tfrac{9}{8}}\langle dd\,|\phi_1\rangle = \sqrt{\tfrac{1}{2}}, \quad (44)$$

given for model B86 in Table 5.

Similar straightforward calculations lead to the matrix elements $\langle\eta_n\eta_n\,|\eta_n\rangle$ and $\langle\eta_s\eta_s\,|\eta_s\rangle$.

References

1. H. Fritzsch, M. Gell-Mann, in Broken scale invariance and the light cone, edited by Iverson and Perlmutter (Gordon and Breach, London 1971); in Proceedings 16th International Conference on High-Energy Physics, Chicago-Batavia, Vol. 2, 135 (1972); H. Fritzsch, M. Gell-Mann, H. Leutwyler, Phys. Lett. B **47**, 365 (1973); S. Weinberg, Phys. Rev. Lett. **31**, 494 (1973); Phys. Rev. D **8**, 4482 (1973); D.J. Gross, F. Wilczek, Phys. Rev. D **8**, 3633 (1973); for a recent review on QCD, see e.g. S. Brodsky, H.-C. Pauli, S. Pinsky, Phys. Rept. **301**, 299 (1998).

2. Y. Nambu, G. Jona-Lasinio, Phys. Rev. **122**, 345 (1961); Phys. Rev. **124**, 246 (1961); G. 't Hooft, Phys. Rev. D **14**, 3432 (1976); Nucl. Phys. B **72**, 461 (1974).
3. For a recent review on experimental tests for QCD, see P.N. Burrows, Precise tests of QCD in e^+e^- annihilation, Report no. MIT-LNS-97-267, SLAC-PUB-7434 (hep-ex/9705013), as well as publications in the proceedings of High-Energy Physics International Euroconference on Quantum Chromodynamics, QCD97, 25th Anniversary of QCD, Montpellier, France, 3–9 July 1997.
4. A. Polleri, R.A. Broglia, P.M. Pizzochero, N.N. Scoccola, Z. Phys. A **357**, 325 (1997); Y. Nemoto, M. Oka, M. Takizawa, Austral. Journ. Phys. **50**, 187 (1997); Phys. Rev. D **54**, 6777 (1996); H.-C. Kim, M.V. Polyakov, A. Blotz, K. Goeke, Nucl. Phys. A **598**, 379 (1996); V. Bernard, A.H. Blin, B. Hiller, Y.P. Ivanov, A.A. Osipov, U-G. Meißner, Ann. Phys. **249**, 499 (1996); B. Bajc, A.H. Blin, B. Hiller, M.C. Nemes, A.A. Osipov, M. Rosina, Nucl. Phys. A **604**, 406 (1996); A. Buck, H. Reinhardt, Phys. Lett. B **356**, 168 (1995).
5. Kurt Langfeld and Mannque Rho, Nucl. Phys. A **596**, 451 (1996).
6. N.A. Törnqvist, Ann. Phys. (N.Y.) **123**, 1 (1979); M. Roos and N. A. Törnqvist, Z. Phys. C **5**, 205 (1980); N. A. Törnqvist, Nucl. Phys. B **203**, 268 (1982).
7. E. van Beveren, G. Rupp, T.A. Rijken, C. Dullemond, Phys. Rev. D **27**, 1527 (1983).
8. E. Eichten, K. Gottfried, T. Kinoshita, K.D. Lane, T.M. Yan, Phys. Rev. D **17**, 3090 (1978); D **21**, 313 (E) (1980); D **21**, 203 (1980).
9. E. Eichten, Phys. Rev. D **22**, 1819 (1980); Nina Byers, Estia Eichten, Phys. Rev. D **42**, 3885 (1990).
10. Nathan Isgur, Phys. Rv. D **60**, 054013 (1999); P.J.A. Bicudo, Phys. Rev. C **60**, 035209 (1999); see also: P.J.A. Bicudo and J.E. Ribeiro, Phys. Rev. D **42**, 1635 (1990).
11. E. van Beveren, T.A. Rijken, K. Metzger, C. Dullemond, G. Rupp, J.E. Ribeiro, Z. Phys. C **30**, 615 (1986).
12. E. van Beveren, C. Dullemond, G. Rupp, Phys. Rev. D **21**, 772 (1980); D **22**, 787 (E) (1980).
13. E. van Beveren, C. Dullemond, T.A. Rijken, Z. Phys. C **19**, 275 (1983); E. van Beveren, C. Dullemond, T.A. Rijken, G. Rupp, Lecture Notes in Physics, **211**, 331 (1984).
14. E. van Beveren, Nucl. Phys. B **21** (Proc. Suppl.), 43 (1991).
15. L. Micu, Nucl. Phys. B **10**, 521 (1969); R. Carlitz, M. Kislinger, Phys. Rev. Lett. **24**, 186 (1970); Phys. Rev. D **2**, 336 (1970); R.P. Feynman, M. Kislinger, F. Ravndal, Phys. Rev. D **3**, 2706 (1971); E.W. Colglazier, J.L. Rosner, Nucl. Phys. B **27**, 349 (1971); W.P. Petersen, J.L. Rosner, Phys. Rev. D **6**, 820 (1972); D **7**, 747 (1973); A. Le Yaouanc, L. Oliver, O. Pène, J.C. Raynal, Phys. Rev. D **8**, 2223 (1973); D **9**, 1415 (1974).
16. K. Abe et al., Phys. Rev. D **59**, 012002 (1999).
17. I. Talmi, Helv. Phys. Acta. **25**, 185 (1952); M. Moshinsky, Nucl. Phys. **13**, 104 (1959); T.A. Brody, M. Moshinsky, Tables of transformation brackets (English/Spanish), (Gordon and Breach, N.Y. 1960); Yu.F. Smirnov, Nucl. Phys. **27**, 177 (1961); M. Baranger, K.T.R. Davies, Nucl. Phys. **79**, 403 (1966).
18. V. Bargmann, M. Moshinsky, Nucl. Phys. **18**, 697 (1960); Nucl. Phys. **23**, 177 (1961); P. Kramer, M. Moshinsky, Nucl. Phys. **82**, 241 (1966); Nucl. Phys. **107**, 481 (1968); Nucl. Phys. **125**, 321 (1969); Group theory of the harmonic oscillator, edited by E.M. Loeb (Academic Press, 1968); M. Moshinsky, Group theory and the many-body problem (Gordon and Breach, N.Y. 1968).
19. J.E. Ribeiro, Phys. Rev. D **25**, 2406 (1982).
20. E. van Beveren, Z. Phys. C **17**, 135 (1983).
21. E. van Beveren, Z. Phys. C **21**, 291 (1984).
22. A.G.M. Verschuren, C. Dullemond, E. van Beveren, Phys. Rev. D **44**, 2803 (1991).
23. N.A. Törnqvist, Z. Phys. C **68**, 647 (1995).
24. N.A. Törnqvist, M. Roos, Phys. Rev. Lett. **76**, 1575 (1996).
25. S. Ishida, M. Ishida, T. Ishida, K. Takamatsu, T. Tsuru, Prog. Theor. Phys. **98**, 621 (1997).
26. D. Black, A. Fariborz, F. Sannino, J. Schechter, Phys. Rev. D **48**, 054012 (1998); M. Napsuciale, Scalar meson masses and mixing angle in a $U(3) \times U(3)$ linear sigma model, hep-ph/9803396.
27. Th. A. Rijken, V.G. J. Stoks, Y. Yamamoto, Phys. Rev. C **59**, 21 (1999).
28. Eef van Beveren, George Rupp, Eur. Phys. J. C **10**, 469 (1999).